Molecular Mechanism for the Radiationless Deactivation of the Intramolecular Charge-Transfer Excited Singlet State of Aminofluorenones through Hydrogen Bonds with Alcohols

Tomoyuki Yatsuhashi,[1] Yuka Nakajima, Tetsuya Shimada, Hiroshi Tachibana, and Haruo Inoue*,[2]

Department of Applied Chemistry, Graduate Course of Engineering, Tokyo Metropolitan University, 1-1 Minami-ohsawa, Hachioji, Tokyo 192-0397, Japan

Received: April 23, 1998; In Final Form: July 28, 1998

The fluorescence quenchings of 12 aminofluorenone (AF) derivatives by ethanol were examined, and the quenching dynamics of the intramolecular charge-transfer excited singlet state of 3-amino-9-fluorenone, as a model molecule, induced by alcohol were studied by steady-state, picosecond fluorescence measurements and quenching experiments. The AF in benzene solution showed substantial red-shiftings of its fluorescence following addition of alcohol. Fluorescence decay analysis revealed that two different relaxed hydrogen-bonded states exist: an emissive state and a nonemissive state. These different states are due to the microscopic anisotropy of the hydrogen bond around the carbonyl oxygen. In the emissive state, the hydroxyl group of the alcohol interacts through an in-plane mode with the carbonyl oxygen of AF, while the alcohol interacts through an out-of-plane mode in the nonemissive state. The out-of-plane mode was shown to be more common with cumene hydroperoxide and diols than with ethanol owing to their steric hindrance in the in-plane mode. Because of its simple structure and charge-transfer nature, AF was found to be the most suitable molecule for examining the microscopic mechanism of radiationless deactivation of the intramolecular charge-transfer excited singlet state through a hydrogen bond.

Introduction

Special attention has focused on processes involving the relaxation of excited molecules as among the most fundamental of molecular processes.[3] Reorganization of solvent molecules surrounding an excited polar molecule has been the topic of considerable study.[4] The general dielectric relaxation behavior of solvent reorganizations has been extensively studied.[5] Solvent reorientation in alcohols can be described by three different relaxation times that reflect three processes: rotation of the C−O bond, rotation of the monomeric molecule, and rotation of the aggregated molecule (with concomitant breaking of the hydrogen bonds in the molecular aggregates).[6] The dielectric relaxation of the excited state was observed within a picosecond time frame. Another important process is the relaxation induced by a specific solvation such as hydrogen-bonding interactions. A recent study showed that a specific solvation contributed substantially to the radiationless deactivation of an excited molecule through intermolecular hydrogen-bonding interactions.[7]

Aminoanthraquinone (AAQ) derivatives in their intramolecular charge-transfer excited singlet states were efficiently deactivated through specific intermolecular hydrogen-bonding interactions with the hydroxyl groups of alcohols used as solvents.[7] The hydrogen bond acts as the effective accepting mode of radiationless transition (internal conversion). The hydrogen-bonding mode is very effective in coupling the excited state and the ground state by virtue of its high frequency. This interpretation was supported by several studies.[8] These past studies are closely related to a fundamental problem not yet fully understood, as to whether the excess energy of an excited molecule is randomly dissipated by the surrounding solvent molecules or inherently flows anisotropically through a selective vibrational mode to the surrounding solvent molecules.

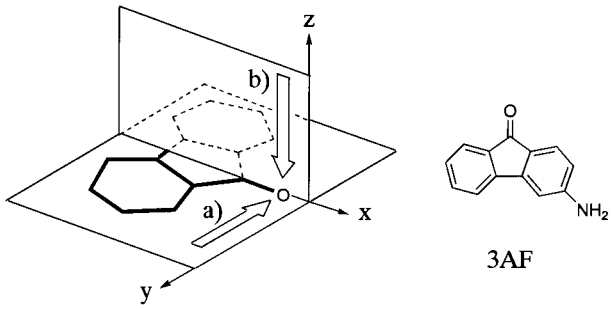

Figure 1. Directions of approach for hydrogen bond formation with a fluorenone carbonyl group: (a) an in-plane-mode approach to the lone pair of the carbonyl; (b) an out-of-plane-mode approach to the π^* orbital of the carbonyl.

From the viewpoint of microscopic specific solvation dynamics, the "molecular mechanism", i.e., anisotropy on a molecular level, is one of the important problems yet to be explained. We previously proposed a molecular mechanism for the radiationless deactivation of excited AAQ through an intermolecular hydrogen bond.[9] Two modes of interaction were postulated: (1) an in-plane mode interaction between the hydroxyl hydrogen of the alcohol and carbonyl oxygen of AAQ and (2) an out-of-plane mode (see Figure 1). Although important new information was obtained, questions remained regarding the two carbonyls within AAQ. Simultaneous intermolecular hydrogen-bonding by both of the two carbonyls might be involved in the deactivation processes. We previously reported that aminofluorenone (AF) derivatives showed very interesting photophysical properties which were strongly dependent on their

* To whom correspondence should be addressed.

10.1021/jp981975x CCC: $15.00
Published on Web 10/17/1998

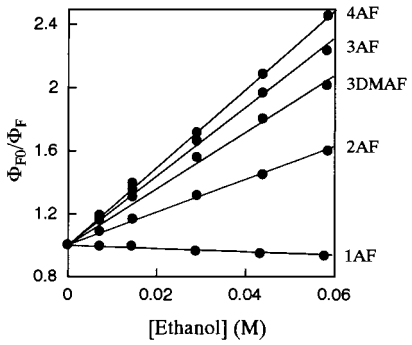

Figure 2. Stern−Volmer plots for the fluorescence quenching of AFs and 3DMAF with ethanol. Plots were obtained using the fluorescence quantum yields.

substitution position.[10] More definitive experimental results would be expected in the case of AFs that have only one carbonyl group.

In this work, we chose AF derivatives as models for molecules which have an intramolecular charge-transfer excited state in order to examine the molecular mechanism of deactivation through an intermolecular hydrogen bond. The mechanism was examined by fluorescence-quenching experiments, using various alcohols. The microscopic molecular quenching mechanism involving anisotropic hydrogen-bonding interactions was then studied.

Experimental Section

Materials. 1-Amino- (1AAQ), 2-amino- (2AAQ), and 2-piperidino-9,10-anthraquinone (2PAQ) were purified as reported previously.[7] 1-Amino- (1AF), 2-amino- (2AF), 3-amino (3AF), and 4-amino-9-fluorenone (4AF), 1-methylamino- (1MAF), 2-methylamino- (2MAF), 3-methylamino- (3MAF), and 4-methylamino-9-fluorenone (4MAF), and 1-(dimethylamino)- (1DMAF), 2-(dimethylamino)- (2DMAF), 3-(dimethylamino)- (3DMAF), and 4-(dimethylamino)-9-fluorenone (4DMAF) were synthesized and purified as reported elsewhere.[10] Ethanol, cumene hydroperoxide (CHP), and dry benzene were prepared as reported.[11] Diols were dried over sodium sulfate and fractionally distilled under reduced pressure. *trans*-1,2-Cyclohexanediol was recrystallized twice from acetone and dried under vacuum at 50 °C for 5 h.

Measurements.[10] Absorption spectra were recorded on a Shimadzu UV-2100PC spectrophotometer, and corrected fluorescence spectra were recorded on a Hitachi F-4010 spectrofluorometer. The fluorescence decay and time-resolved fluorescence spectra were measured using a picosecond fluorescence lifetime measurement system under photon-counting conditions (Hamamatsu, C4334 streak scope, connected to a CHROMEX 250IS polychromater) with a Hamamatsu PLP-02 semiconductor laser (420 nm, fwhm 20 ps, 1.19 mW, 1 MHz) and an EKSPLA PV-401 optical parametric generator (420−560 nm, fwhm 25 ps, >1 mJ, 5 Hz) pumped by the third harmonic radiation of a Nd^{3+} YAG laser, EKSPLA PL2143B (355 nm, 25 ps fwhm, 15 mJ), or by the third harmonic of the PL2143B itself. The laser flux was reduced with neutral density filters to avoid multiphoton absorption processes and nonlinear effects in the latter case. A single picosecond optical pulse from the regenerative amplifier of the PL2143B laser was extracted by an InGaAs photodiode (Hamamatsu, G3476-05) and used as a pretrigger for the streak scope. This method turned out to be very useful for avoiding trigger jitter problems with the streak scope, because it caused no additional jitter. Fluorescence time profiles were fitted by a convolution method. All measurements were carried out under air at 296 K.

TABLE 1: Apparent Stern−Volmer Constants from Steady-State Fluorescence-Quenching Experiments Using Ethanol

	K_{SV} (M^{-1})[a]	τ (ns)[b]	k_q (10^9 M^{-1} s^{-1})
1AAQ	1.5	1.9	0.80
2AAQ	36.6	7.5	4.9
2PAQ	31.4	9.5	3.3
fluorenone	(−5.9)[c]	2.8	*c*
1AF	(−1.2)[c]	1.4	*c*
2AF	10.4	0.80	13
3AF	21.8	11	2.0
4AF	24.7	9.2	2.7
1MAF	0	2.8	0
2MAF	10.3	0.63	16
3MAF	18.2	9.4	1.9
4MAF	37.1	8.4	4.4
1DMAF	0	0.02/2.2	0
2DMAF	10.3	0.79	13
3DMAF	18.0	11	1.7
4DMAF	28.9	10	2.9

[a] The Stern−Volmer constant, K_{SV}, was obtained for the fluorescence quantum yield assuming a linear correlation (eq 1). [b] Fluorescence lifetime in benzene; ref 10. [c] Fluorescence was enhanced by the addition of ethanol.

Results and Discussions

Fluorescence Quenching of AF by Alcohol. In ethanol, the fluorescence quantum yields of AAQ and AF are 2 orders less than those in benzene and 1 order less than those in acetonitrile.[7,10] It was concluded that the excited singlet states of AAQ and AF were effectively quenched by ethanol.[7,10] The fluorescence-quenching experiments in benzene were carried out to explore the molecular mechanisms of the quenching phenomena. First of all, the steady-state fluorescence-quenching experiments using ethanol, as a typical monoalcohol, were examined and the apparent Stern−Volmer constants for the fluorescence quantum yields were calculated using eq 1, where Φ_{F_0}, Φ_F, k_q,

$$\Phi_{F_0}/\Phi_F = 1 + k_q\tau[\mathrm{ROH}] = 1 + K_{SV}[\mathrm{ROH}] \qquad (1)$$

τ, K_{SV}, and [ROH] are the fluorescence quantum yields in the absence and presence of a quencher, quenching rate constant, fluorescence lifetime in benzene, Stern−Volmer constant, and concentration of ROH (alcohol), respectively. The fluorescence was quenched by the addition of ethanol except for fluorenone and 1AF. The correlation coefficient for each Stern−Volmer plot was greater than 0.995, assuming a linear correlation for any sensitizer, though the plots of the 3-aminofluorenone derivatives appeared to have a slight curvature (Figure 2). The obtained K_{sv} values are given in Table 1.

The fluorescence of fluorenone and 1AF was enhanced by the addition of ethanol, and the fluorescence was red-shifted as in the case of 1AF−trifluoroethanol reported by Moog et al.[11] 1MAF and 1DMAF were not quenched, but fluorescence was red-shifted. Recently, the fluorescence quenching of fluorenone by alcohol in DMF and in CH_2Cl_2 was reported by Biczók et al.[12] However, the fluorescence quenching of fluorenone cannot be observed in a nonpolar solvent owing to the close proximity of n, π * and π, π * states and to the delicate positioning of the n, π* triplet state.[10,13] This is also true for 1AF and 1MAF, where the dominant mode of radiationless transition is intersystem crossing.[10] In the case of 1DMAF, the relaxation process with ethanol cannot compete with the very fast deactivation

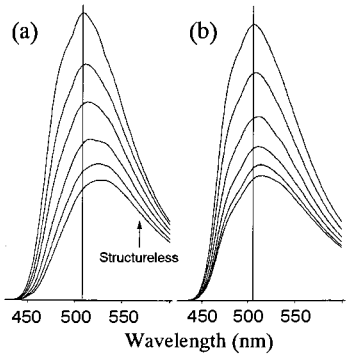

Figure 3. Fluorescence spectral changes of 3AF in the presence of (a) ethanol and (b) 1,3-propandiol. [ethanol] = 0−0.065 M and [propanediol] = 0−0.013 M. The structure of 3AF is also shown.

process involving twisted intramolecular charge-transfer state formation.[10] 2-Aminofluorenone derivatives were significantly quenched by ethanol on the order of 10^{10} M^{-1} s^{-1}. The fluorescence quenching of 4-aminofluorenone derivatives was similar to those of 2AAQ and 2PAQ.[9] The slight difference in the quenching rate constants between 4MAF and 4DMAF may be attributed to their charge-transfer characteristics, which are affected by their structural differences. The former has a planar conformation and the latter has a perpendicular conformation of the dimethylamino group with the fluorenone nucleus in the ground state.[10] 3-Aminofluorenone derivatives showed unique quenching phenomena that warranted further study. The Stern−Volmer plots appeared to have a slight curvature. This nonlinearlity in the Stern−Volmer analysis will give us additional information about the relaxed state. The details are discussed in a later section.

Fluorescence Spectral Shifts. The addition of ethanol resulted in not only a decrease in the fluorescence intensity but also a red-shifting of the fluorescence as was the case for the AAQs.[9] As observed in the time-resolved fluorescence spectra described below, the red shifts of the fluorescence were due to the new emissive species that appeared in the long-wavelength region. The shifts depended on the sensitizers, and the degree of shiftings followed the order 4AF, 2AAQ > 3AF > 2AF > 2PAQ > 1AAQ. The shape of the spectra of AAQ derivatives did not appear to change much upon the addition of alcohol owing to its structureless spectra, and only λ_{max} shifts were observed.[9] However, for 3-aminofluorenone derivatives, which have weak fluorescence structures, changes in the spectral shape were clearly observed (Figure 3). A notable difference was observed between ethanol and an alkanediol such as 1,3-propanediol. Upon the addition of ethanol, the weakly structured fluorescence spectrum of 3AF became structureless with a concurrent red shift of λ_{max}. A similar tendency was less evident in the case of 1,3-propanediol. Although this change in the spectrum is noteworthy, the association of alcohols needs to be discussed first. The self-association of alcohol has been widely studied.[14] The formation of dimers and even tetramers is appreciable at high concentrations of ethanol, while the monomer is dominant at low concentrations (<0.06 M in CCl_4).[15] The latter corresponds to the highest concentration used in our experiments in benzene. The monomer percentage is at least 94% in CCl_4, at an ethanol concentration of 0.06 M.[15] The aggregation of ethanol should be less significant in benzene, where the monomeric hydroxyl group is better stabilized by the $\pi\cdots$HOR interaction. The alkanediols, $HO(CH_2)_nOH$ (n = 2−4), form intramolecular hydrogen bonds, while the contribution of intermolecular hydrogen bonds (self-association) is negligible in a dilute solution.[16] The data obtained in this study

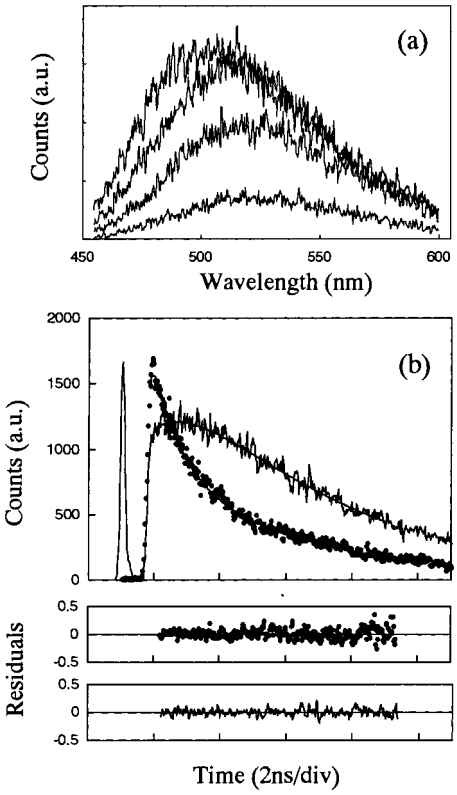

Figure 4. (a) Time-resolved fluorescence spectra of 3AF in the presence of 0.06 M ethanol at 0 s, 1, 3, and 8 ns after excitation. Gate width was 0.4 ns. (b) The upper panel shows the fluorescence decays of 3AF in the presence of 0.06 M ethanol in the short (dots, 460−480 nm) and in the long (line, 555−575 nm) wavelength region, along with the instrument response function, which has been shifted in time to provide a clearer presentation. The lower panels show the residuals for the decays when simultaneously fit to the functional forms in eqs 10 and 11.

were analyzed by assuming that the alcohols exist as monomers under the experimental conditions.

These results strongly suggest that the contribution of the new structureless emission in the long-wavelength region is substantial in the presence of ethanol, while its contribution is small in the presence of 1,3-propanediol. Though similar effects on the λ_{max} shifts were also observed for the cases of AAQ,[9] the difference was more explicitly reflected in the shape of the fluorescence spectra in the case of 3AF. Other alkanediols ($HO(CH_2)_nOH$, n = 2−7) exhibited structured spectra similar to those for 1,3-propanediol. In the case of cumene hydroperoxide (CHP), on the other hand, the spectrum did not show any significant broadening. Obviously, the alcohols examined here could be classified into two groups: (1) alcohols such as ethanol that quench the fluorescence of 3AF with a substantial red shift of λ_{max} that results in spectrum broadening and (2) alcohols such as alkanediols and CHP that quench the fluorescence with minor shifting and little spectrum broadening. These phenomena should directly reflect the degree of contribution of the new broad emission in the long-wavelength region, and their differences should be closely related to the microscopic molecular mechanism of fluorescence quenching.

Time-Resolved Fluorescence Spectra of 3AF. To obtain more information on the molecular mechanism of fluorescence quenching, its dynamic behavior was further studied. The time-resolved fluorescence spectra of 3AF in the presence of 0.06 M ethanol, as a typical case, are shown in Figure 4a. A new emissive species in the longer wavelength region is clearly

TABLE 2: Rate Constants for 3AF Estimated from the Time-Resolved and Steady-State Fluorescence-Quenching Experiments[a]

quencher	MS(O*H*) (Å^2)[b]	k_1 (10^9 M^{-1} s^{-1})[c]	$k' + \beta k_{-1}$ (10^8 s^{-1})[d]	$k' + k_{-1}$ (10^8 s^{-1})[e]	αk_{-1} (10^8 s^{-1})[e]	spectral changes[f]
ethanol	5.82	7.2	2.3	5.9	3.6	+
cumene hydroperoxide	6.23	8.5	3.5	5.3	1.8	−
trans-1,2-cyclohexanediol	8.3	13	3.4	4.4	1.0	−
1,3-propanediol	11.2	20	2.4	3.8	1.4	−

[a] The fluorescence decay profile (555−575 nm) was analyzed. [b] Contact molecular surface area of the hydroxyl hydrogen of the quencher (probe radius = 1.4 Å). The details were described in ref 9. [c] Obtained from $\lambda_1 + \lambda_2$ vs [ROH] plot (eq 12). [d] Obtained from $\lambda_1\lambda_2$ vs [ROH] plot (eq 13). [e] Obtained from $k' + \beta k_{-1}$ and a in eq 14 as described in the text. [f] Fluorescence spectral changes, describing the spectral broadening and spectral shift (+, fluorescence spectrum showed broadening and λ_{max} was significantly shifted to the red upon addition of the quencher; −, a small broadening of the fluorescence spectrum was observed and λ_{max} was slightly shifted upon addition of the quencher).

observed. The fluorescence decay profiles are shown in Figure 4b. A clear rise and decay profile is observed in the longer wavelength region. The profile is more well-defined than in the case of the AAQs.[9] Two emissive states such as the original fluorescent state in benzene (S_1) and a relaxed emissive state (S_1(RX)) were assumed. Furthermore, another nonemissive state leading to an efficient deactivation is also assumed in the following results and discussion as in the case of the AAQs.[9] The relaxed emissive state in benzene is assigned as the corresponding excited state of the hydrogen-bonded form with ethanol in the ground state as described below, but deactivation from the state is too inefficient (on the order of 10^8 s^{-1}) compared with that in neat ethanol (3.4×10^9 s^{-1})[10] as demonstrated below (Table 2). The fluorescence time profile of 3AF in neat ethanol has no rise time, and the emissive state is assigned as a fully hydrogen-bonded relaxed excited state.[10] Assuming that the two relaxed hydrogen-bonded emissive states in benzene and ethanol are the same species, the large discrepancy between the two deactivation rate constants cannot be easily explained by a difference in solvent polarity. Some other factors must be involved in the deactivation in neat ethanol. Since a solute molecule is completely surrounded by ethanol molecules in neat ethanol, several ethanol molecules presumably interact with 3AF in several modes leading to an efficient deactivation. Another mode of interaction with ethanol leading to an efficient deactivation other than that involving the emissive state is thus assumed in ethanol. This leads one to postulate that, even in benzene, the interaction of ethanol molecules involves not only the emissive species but also the nonemissive one, which results in efficient deactivation.

The fluorescence decay kinetics were, thus, analyzed by the decay processes of eqs 2−9, including two pathways: (1) relaxation to an emissive state (eq 3) and (2) effective internal conversion to the ground state via a nonemissive state (S_1(RX′), eq 4). Here, where I, αk_1, βk_1, k_r, k_{nr}, k_r', k_{nr}', k_{-1}, and [ROH]

	Process		Rate constant	
$S_0 + h\nu$	$\xrightarrow{I}$	S_1		(2)
S_1 + ROH	$\longrightarrow$	S_1(RX)	αk_1 [ROH]	(3)
S_1 + ROH	$\xrightarrow{-S_1(RX')}$	S_0	βk_1 [ROH]	(4)
S_1	$\longrightarrow$	$S_0 + h\nu'$	k_r	(5)
S_1	$\longrightarrow$	S_0	k_{nr}	(6)
S_1(RX)	$\longrightarrow$	$S_0 + h\nu''$	k_r'	(7)
S_1(RX)	$\longrightarrow$	S_0	k_{nr}'	(8)
S_1(RX)	$\longrightarrow$	S_1	k_{-1}	(9)

are the light absorption rate, the forward rate constant to the S_1(RX) state from S_1, the radiationless deactivation rate constant to the ground state via the nonemissive state (S_1(RX′)) caused by alcohol, the radiative and radiationless rate constants from the S_1 state in benzene, the radiative and radiationless rate constants of the S_1(RX) state, the backward rate constant from the S_1(RX) state to S_1, and the concentration of alcohol, respectively. $\alpha + \beta = 1$. The populations of each state are written as eqs 10 and 11,[17] where $k = k_r + k_{nr}$ and $k' = k_r' +$ k_{nr}'. A, B, and C are functions of the time constants λ_1 and λ_2 and of the concentration [ROH]. The concentration dependences of the time constants, λ_1 and λ_2, are then written as eqs 12 and 13.[17] As indicated in Figure 4, the original fluorescence

$$[S_1]t = A\exp(-\lambda_1 t) + B\exp(-\lambda_2 t) \quad (10)$$

$$[S_1(RX)] = C\{\exp(-\lambda_1 t) - \exp(-\lambda_2 t)\} \quad (11)$$

$$\lambda_{2,1} = 0.5\{k + k_1[ROH] + k_{-1} + k' \pm \sqrt{(k + k_1[ROH] - k_{-1} - k')^2 + 4\alpha k_1 k_{-1}[ROH]}\}$$

$$\lambda_1 + \lambda_2 = k + k' + k_{-1} + k_1[ROH] \quad (12)$$

$$\lambda_1\lambda_2 = k(k' + k_{-1}) + k_1(k' + \beta k_{-1})[ROH] \quad (13)$$

from the S_1 state in the shorter wavelength region and the new emission from S_1(RX) in the longer wavelength region could be superimposed upon each other over the entire observation region. Since the new emission contributes more in the longer wavelength region than in the shorter one, the rise and decay profiles in the longer wavelength region (555−575 nm) were analyzed in order to avoid the low signal-to-noise ratio in the shorter wavelength region. Typical examples of plots of eqs 12 and 13 are shown in Figure 5a. Ethanol was used as a typical alcohol, and a good linear correlation was obtained. Similar analyses were performed and good correlations were derived for CHP, *trans*-1,2-cyclohexanediol, and 1,3-propanediol. These results are summarized in Table 2. Since the intercepts might contain errors, the rate constants, k_1 and ($k' + \beta k_{-1}$), were obtained from the slopes of the plots of eqs 12 and 13, respectively.

A striking difference was found in k_1: the diols apparently have larger values than the calculated diffusion-limited rate constant (1×10^{10} M^{-1} s^{-1}).[18] For example, the propanediol value is almost 2 times larger, while those for ethanol and CHP approximate the diffusion-controlled rate constant. The quenching constants are well-correlated with the contact molecular surface area of the hydroxyl hydrogen of alcohols (MS(O*H*)),[9,19] an exposed area being accessible by the carbonyl oxygen atom. The MS(O*H*) of propanediol is 11.2 Å^2, almost twice that of ethanol (5.82 Å^2) (Table 2). These results clearly show that diols act as bifunctional quenchers.

New Emission in the Long-Wavelength Region. When an excess of ethanol was added to the benzene solution of 3AF, a

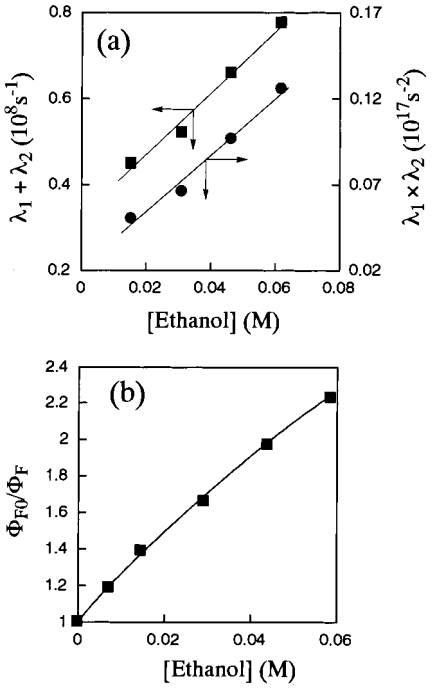

Figure 5. (a) Kinetic analysis of 3AF fluorescence time constants in the presence of ethanol using eqs 12 and 13. (b) Nonlinear Stern−Volmer plot for the fluorescence quenching of 3AF with ethanol. The solid line was obtained from a curve-fit of the data using eq 14.

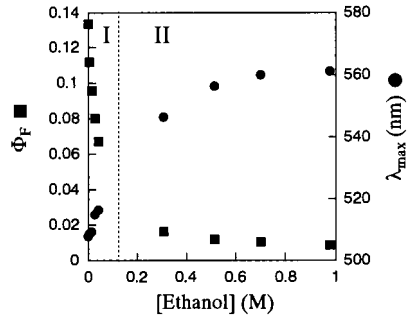

Figure 6. Fluorescence quantum yield (■) and fluorescence λ_{max} (●) of the ground-state complex between 3AF and ethanol. 3AF was excited at its absorption λ_{max} (395 nm) in benzene in region I, where [ethanol] = 0−0.06 M. The hydrogen-bonded complex between 3AF and ethanol was excited at 480 nm in region II, where [ethanol] = 0.3−1.0 M.

new absorption band appeared in the long-wavelength region with an isosbestic point at 389 nm. The new absorption band could be assigned as the ground-state hydrogen-bonded complex between 3AF and ethanol, as observed for the AAQs.[9] The 3AF−ethanol association constant is 0.90 [M^{-1}], estimated from the absorption spectral changes and assuming a 1:1 complex formation. The ground-state hydrogen-bonded complex, in the presence of an excess of ethanol up to 1.0 M, was excited at λ = 480 nm, where the absorption for 3AF is very small. Broader, structureless fluorescence spectra were thus observed in the longer wavelength region compared to the original fluorescence of 3AF in benzene. The additional ethanol induced the λ_{max} red-shifting as indicated in Figure 6. The fluorescence quantum yield also varied according to the ethanol concentration, decreasing to around $\Phi_F = 0.01$ at 1.0 M ethanol. The spectral shape and apparent λ_{max} are similar to those for the new emission in the long-wavelength region observed for both the steady-state and time-resolved fluorescence spectra. The new emission in the long-wavelength region observed in the dynamic quenching of the 3AF fluorescence can thus be assigned as fluorescence from the hydrogen-bonded complex. The relaxed emissive state responsible for the new emission is probably the corresponding excited state of the ground-state hydrogen-bonded complex, although the formation of the ground-state hydrogen-bonded complex is almost negligible at the low ethanol concentrations (0−0.06 M) used in the present study. The nuclear configuration of the relaxed emissive state should be quite similar to that of the ground-state hydrogen-bonding complex. Since the hydrogen-bonding interaction between the hydroxyl hydrogen and the carbonyl oxygen of ground-state 3AF is accepted to be through the nonbonding orbital of oxygen (Figure 1), relaxation to the emissive state (S_1(RX)) should be induced by an in-plane-mode attack of alcohol on the carbonyl oxygen. Another relaxation to the nonemissive state involving an efficient deactivation is, thus, speculated to be induced by an out-of-plane-mode attack of alcohol through the π^* orbital of the carbonyl, as also postulated for the AAQs.[9] Hydrogen-bond formation between ethanol and the π^* orbital on the carbonyl group of the fluorenone radical anion[20] and the benzophenone radical anion[21] has also been postulated. A semiempirical molecular orbital calculation also predicts that an out-of-plane-mode interaction is favored in the excited state.[22]

Kinetic Analysis of Fluorescence Quenching. In the steady-state fluorescence-quenching experiments described earlier, the Stern−Volmer plots showed a slight curvature only for 3-aminofluorenone derivatives with alcohols. According to the processes depicted in eqs 2−9, the Stern−Volmer equation can be written in a more complex formalism involving quenching as the nonlinear form of eq 14,[23] where $a = k_1(k' + \beta k_{-1})/(k' + k_{-1})$ and $b = \alpha k_1 k_r'/[k_r (k' + k_{-1})]$.

$$\frac{\Phi_{F_0}}{\Phi_F} = \frac{1 + \frac{a}{k}[\mathrm{ROH}]}{1 + b[\mathrm{ROH}]} \qquad (14)$$

For AAQs and aminofluorenones, other than the 3-aminofluorenone derivatives, the Stern−Volmer plots in Figure 2 appear fairly straight, since the fluorescence quantum yield of the emissive state is relatively small (it would be 2 orders smaller than the original fluorescence) and the term b in eq 14 is negligibly small. On the other hand, nonlinear Stern−Volmer plots were obtained for 3-aminofluorenone derivatives, where a substantial contribution owing to the new emission from the relaxed emissive state (S_1(RX)) in the long-wavelength region was observed. The b term in eq 14 is significant in these cases. More information about the emissive states could, thus, be obtained by analyzing the nonlinear Stern−Volmer plot of 3AF. A curve-fit using eq 14 of the nonlinear plot of 3AF with ethanol is shown in Figure 5b, where the terms a/k and b were determined as 31 M^{-1} and 4.5 M^{-1}, respectively. These values represent the fluorescence quantum yield at an infinite ethanol concentration: $\Phi_F(\infty) = (\Phi_{F_0} bk)/a = 0.02$, since $\Phi_{F_0} = 0.13$.[10] The quantum yield $\Phi_F(\infty)$ is comparable to the saturated value of the apparent quantum yield of fluorescence ($\Phi = 0.01$) shown in Figure 6.[24]

In eqs 12−14, we have five unknown parameters such as k_1, k', k_{-1}, α ($\beta = 1 - \alpha$), and k_r', but we can only determine four values such as k_1 and $k' + \beta k_{-1}$ from eqs 12 and 13 and a and b from eq 14. One cannot determine all of the parameters in this situation. We now try to estimate k' and α. With a combination of $k_1(k' + \beta k_{-1})$ and a, we can determine the value of $k' + k_{-1}$ and obtain $(1 - \beta)k_{-1}$ ($=\alpha k_{-1}$) by calculating $[(k' + \beta k_{-1})(k_1 - a)]/a$. These derived values are compared in Table 2. Since the energy differences between the original fluorescent state (S_1) and the relaxed emissive state (S_1(RX)) are supposedly

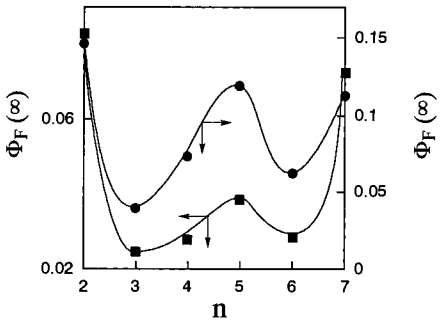

Figure 7. Correlation between the fluorescence quantum yield at infinite diol concentration ($\Phi_F(\infty)$) and methylene chain length (n) of linear diols: (■) 3AF; (●) 3DMAF. $\Phi_F(\infty)$ was calculated using a/k and b from eq 14 and Φ_{F_0} (0.13).

quite similar among the studied alcohols (as judged from nearly identical λ_{max} values for the new emission in the time-resolved fluorescence spectra), k_{-1} is assumed to be constant among the alcohols. Assuming k_{-1} is constant among the alcohols studied, we can make rough estimates of k' and α.

This led to some very important results. The values of $k' + k_{-1}$ did not vary significantly among the alcohols examined, indicating the deactivations (k') from the relaxed emissive states $S_1(RX)$, which could be affected by the nature of the intermolecular hydrogen bond in the in-plane mode, are also similar. Interestingly, the value of αk_{-1} was appreciably larger for ethanol than for the other alcohols. Thus, the relative value of αk_{-1} directly reflects the value of α ($=1 - \beta$), the fraction of collisional attacks by alcohol on 3AF that leads to a relaxed emissive state relative to another attack leading to a nonemissive state (fraction β). The larger αk_{-1} value for ethanol clearly indicates either (1) that ethanol prefers the former attack or (2) that other alcohols prefer the latter attack. As shown in Table 2, the magnitude of αk_{-1} (which is largest for ethanol) is well-correlated with fluorescence spectral characteristics such as spectrum broadening and λ_{max} red-shifting (which are most notable for ethanol). Since ethanol is the smallest molecule among the examined alcohols, it should suffer the least steric hindrance for an in-plane-mode attack on the carbonyl oxygen, where two hydrogen atoms in the 1- and 8-positions of the fluorenone nucleus could cause the hindrance effect. The larger αk_{-1} value for ethanol compared to the other alcohols, thus, strongly suggests the second case described above. CHP, *trans*-1,2-cyclohexanediol, and 1,3-propanediol are less favorable against an in-plane-mode attack, presumably owing to steric hindrance against the fluorenone nucleus, than an out-of-plane-mode attack, where little steric hindrance is involved.

Quenching by Diols as a Model System with Multiple Hydroxyl Groups. As noted above, deactivation of the excited singlet state of 3AF is far more efficient in neat ethanol than in benzene. Because several ethanol molecules surround 3AF, both out-of-plane-mode and in-plane-mode interactions may occur simultaneously in neat ethanol. To simulate the conditions in neat ethanol, fluorescence-quenching experiments using alkanediols, $HO(CH_2)_nOH$ ($n = 2-7$), which possess two hydroxyl groups, were performed in benzene. The results were interesting. The a/k and b terms in eq 14 were estimated for each diol using nonlinear Stern−Volmer plots similar to those in Figure 5. The fluorescence quantum yields at infinite diol concentration, $\Phi_F(\infty)$, were calculated from those values and plotted in Figure 7.[24] Two minimums, at propanediol ($n = 3$) and hexanediol ($n = 6$), were clearly observed for the $\Phi_F(\infty)$ values. As proposed for the AAQs, where only propanediol was examined, the first hydroxyl group of the diol interacts through an in-plane mode while the second hydroxyl group attacks the carbonyl in an out-of-plane mode as shown in Figure 8 ($S_1(RX'')$). Ring formation of the two hydroxyl groups with the carbonyl might be more favorable for propanediol and hexanediol. Intramolecular hydrogen-bond formation was reported for alkanediols of $n = 2-4$.[16] They form five ($n = 2$), six ($n = 3$), and seven ($n = 5$) membered rings within the molecule. This precyclized diol structure may be more amenable to attachment with the carbonyl oxygen of 3AF. Although the possibility of ring formation is uncertain, our observations with the alkanediols suggest that further studies are warranted.

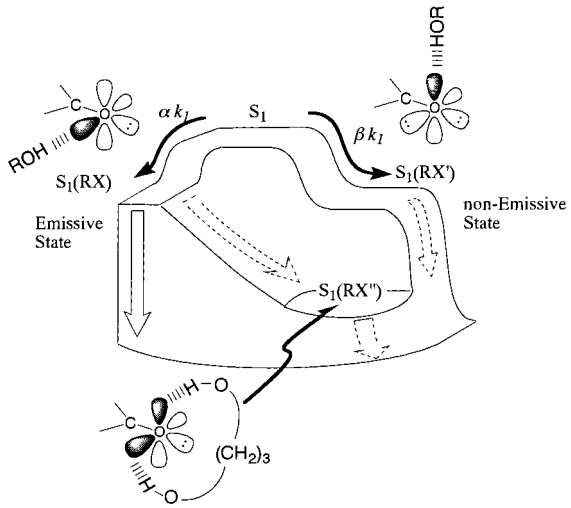

Figure 8. Oversimplified picture of the molecular mechanism for the fluorescence quenching of aminofluorenone. S_1, $S_1(RX)$, $S_1(RX')$, and $S_1(RX'')$ represent the original fluorescent state in benzene, relaxed emissive state, relaxed nonemissive state, and relaxed nonemissive state with two modes of deactivation.

Many interesting examples of specific hydrogen-bonding interactions in the excited state have appeared.[25] The present study is a typical example of radiationless deactivation through a specific solvation. Further study is needed to show how the excitation energy dissipates through anisotropic hydrogen-bond interactions. A possible vibrational mode for radiationless deactivation through an out-of-plane interaction might involve a bending motion of the carbonyl group. Molecular dynamics simulation and time-resolved transient Raman scattering spectroscopy are powerful tools that could be used for future microscopic studies of anisotropy in radiationless deactivation.

Conclusion

The molecular mechanism for radiationless deactivation caused by specific solvation was studied in order to gain insight into the microscopic processes regarding (1) which direction a quencher interacts, (2) which vibrational mode participates in the deactivation, (3) the extent to which the excess energy is dissipated, and (4) why those processes occur. The excited singlet state of aminofluorenone derivatives, which have only one carbonyl group available as a hydrogen-bonding site, was effectively quenched by ethanol. The experimental results and the data analysis plots were more detailed for 3AF than for the AAQs, a consequence of 3AF having only one carbonyl group. The sudden appearance of a giant dipole upon excitation to the intramolecular charge-transfer excited state induces either an in-plane-mode attack that leads to a relaxed emissive state ($S_1(RX)$) or an out-of-plane-mode attack that results in a nonemissive state ($S_1(RX')$) which involves efficient deactivation.

Acknowledgment. We thank Dr. Jonas Kolenda of Tokyo Instruments Inc. and Mr. Haruhisa Saito of Hamamatsu Pho-

tonics K.K. for their kind contributions to our laser system. This work was partly supported by a Grant-in Aid from the Ministry of Education, Science, Sports, and Culture of Japan.

References and Notes

(1) Present address: Department of Chemistry, Faculty of Science, Osaka City University, 3-3-138 Sugimoto, Sumiyoshi, Osaka 558-8585, Japan. E-mail: tomo@sci.osaka-cu.ac.jp.

(2) E-mail: inoue-haruo@c.metro-u.ac.jp.

(3) Maroncelli, M.; Macinnis, J.; Fleming, G. R. *Science* **1989**, *243*, 1674. Horng, M. L.; Gardecki, J. A.; Papazyan, A.; Maroncelli, M. *J. Phys. Chem.* **1995**, *99*, 17311.

(4) Fonseca, T.; Ladanyi, B. M. *J. Phys. Chem.* **1991**, *95*, 2116. Phelps, D. K.; Weaver, M. J.; Ladanyi, B. M. *Chem. Phys.* **1993**, *176*, 575.

(5) Maroncelli, M. *J. Chem. Phys.* **1991**, *94*, 2084. Reid, P. J.; Barbara, P. F. *J. Phys. Chem.* **1995**, *99*, 3554. Stratt, R. M.; Maroncelli, M. *J. Phys. Chem.* **1996**, *100*, 12981.

(6) Garg, S. K.; Smyth, C. P. *J. Phys. Chem.* **1965**, *69*, 1294. Su, S. G.; Simon, J. D. *J. Phys. Chem.* **1987**, *91*, 2693.

(7) Inoue, H.; Hida, M.; Nakashima, N.; Yoshihara, K. *J. Phys. Chem.* **1982**, *86*, 3184.

(8) (a) Ritter, J.; Borst, H. U.; Lindner, T.; Hauser, M.; Brosig, S.; Bredereck, K.; Steiner, U. E.; Kühn, D.; Kelemen, J.; Kramer, H. E. A. *J. Photochem. Photobiol. A* **1988**, *41*, 227. Borst, H. U.; Kelemen, J.; Fabian, J.; Nepras, M.; Kramer, H. E. A. *J. Photochem. Photobiol. A* **1992**, *69*, 97. (b) Srivatsavoy, V. J. P.; Venkataraman, B.; Periasamy, N. *J. Photochem. Photobiol. A* **1992**, *68*, 169. *Proc.—Indian Acad. Sci., Chem. Sci.* **1992**, *104*, 731. (c) Flom, S. R.; Barbara, P. F. *J. Phys. Chem.* **1985**, *89*, 4489. (d) Jones, G., II.; Feng, Z.; Bergmark, W. R. *J. Phys. Chem.* **1994**, *98*, 4511. (e) Lin, S.; Struve, W. S. *J. Phys. Chem.* **1991**, *95*, 2251.

(9) Yatsuhashi, T.; Inoue, H. *J. Phys. Chem. A* **1997**, *101*, 8166.

(10) Yatsuhashi, T.; Nakajima, Y.; Shimada, T.; Inoue, H. *J. Phys. Chem. A* **1998**, *102*, 3018.

(11) Moog, R. S.; Burozski, N. A.; Desai, M. M.; Good, W. R.; Silvers, C. D.; Thompson, P. A.; Simon, J. D. *J. Phys. Chem.* **1991**, *95*, 8466.

(12) Biczók, L.; Bérces, T.; Linshitz, H. *J. Am. Chem. Soc.* **1997**, *119*, 11071.

(13) Biczók, L.; Bérces, T.; Márta, F. *J. Phys. Chem.* **1993**, *97*, 8895.

(14) Rochester, C. H. In *The chemistry of the hydroxyl group. Part 1*; Patai, S., Ed.; Interscience: London, 1971; Chapter 7.

(15) Saunders; M.; Hyne, J. B. *J. Chem. Phys.* **1958**, *29*, 1319. Fletcher, A. N.; Heller, C. A. *J. Phys. Chem.* **1967**, *71*, 3742.

(16) Kuhn, L. P. *J. Am. Chem. Soc.* **1952**, *74*, 2492. Foster, A. B.; Haines, A. H.; Stacey, M. *Tetrahedron* **1961**, *16*, 177. Mori, N.; Omura, S.; Tsuzuki, Y. *Bull. Chem. Soc. Jpn.* **1965**, *38*, 1631.

(17) The usual two-state kinetics were modified for two emissive states and one nonemissive state model. The usual kinetics are described in: Birks, J. B. *Photophysics of Aromatic Molecules*; Wiley: London, 1970; Chapter 7.

(18) Murov, S. L.; Carmichael, I.; Hug, G. L. *Handbook of Photochemistry*, 2nd ed.; Marcel Dekker: New York, 1993; Section 7.

(19) Contact molecular surface area is defined as the van der Waals molecular surface area that is exposed outside and is accessible by another specific probe atom or molecule. A specific probe atom that has a van der Waals radius is rolled on the surface of the corresponding molecule in an optimized geometry. The details of the contact molecular surface area (MS-(O*H*)) was described in ref 9.

(20) Ichikawa, T.; Ueda, K.; Yoshida, H. *Bull. Chem. Soc. Jpn.* **1991**, *64*, 2695.

(21) Tachikawa, H. *J. Phys. Chem.* **1996**, *100*, 17090.

(22) The semiempirical molecular orbital calculation (MOPAC93, PM3) of the 3AF−methanol system demonstrated the existence of anisotropy of the hydrogen bond. The only hydrogen bond on the lone pair of oxygen (Figure 1a) was stable in the ground state, while the energy minimum on the π^* orbital (Figure 1b) was found in the excited state also: Tachibana, H.; Tajima, M.; Yatsuhashi, T.; Nakajima, Y.; Inoue, H. *Abstracts of Papers*, 72nd National Meeting of the Chemical Society of Japan, Tokyo, 1997; Abstract I, p 171.

(23) The steady-state two state kinetics were described in: Mataga, N.; Kubota, T. *Molecular Interactions and Electronic Spectra*; Marcel Dekker: New York, 1970; Chapter 7.

(24) $\Phi_{F_0}(\infty)$ is calculated as 0.02 with the value Φ_{F_0}/Φ_F at an infinite ethanol concentration, equal to $a/(kb)$ in eq 14, and Φ_{F_0} (0.13 in benzene).

(25) (a) Miyasaka, H.; Wada, K.; Ojima, S.; Mataga, N. *Isr. J. Chem.* **1993**, *33*, 183. Miyasaka, H.; Tabata, A.; Kamada, K.; Mataga, N. *J. Am. Chem. Soc.* **1993**, *115*, 7335. Miyasaka, H.; Tabata, A.; Ojima, S.; Ikeda, N.; Mataga, N. *J. Phys. Chem.* **1993**, *97*, 8222. (b) Safarzadeh-Amiri, A. *J. Phys. Chem.* **1989**, *93*, 4999. Brun, A. M.; Harriman, A.; Tsuboi, Y.; Okada, T.; Mataga, N. *J. Chem. Soc., Faraday Trans.* **1995**, *91*, 4047. (c) Sessler, J. L.; Wang, B.; Harriman, A. *J. Am. Chem. Soc.* **1995**, *117*, 704. (d) Biczók, L.; Gupta, N.; Linschitz, L. *J. Am. Chem. Soc.* **1997**, *119*, 12601. Gupta, N.; Linschitz, H.; Biczók, L. *Fullerene Sci. Technol.* **1997**, *5*, 343, Biczók, L.; Linschitz, L. *J. Phys. Chem.* **1995**, *99*, 1843.